Title
Robust Hybrid Kalman Filter for a Class of Nonlinear Systems

ISBN
9781538654286

Authors
Malladi, Bharani P
Sanfelice, Ricardo G
Butcher, Eric A

Publication Date
2018-06-01

DOI
10.23919/acc.2018.8431473

Peer reviewed

Robust Hybrid Kalman Filter for a Class of Nonlinear Systems

Bharani P. Malladi, Ricardo G. Sanfelice, and Eric A. Butcher

Abstract— **Motivated by real-world applications with intermittent sensor data, an extended Kalman filter is formulated as a hybrid system and constructive conditions on its parameters guaranteeing an asymptotic stability property are provided. The dynamical properties of the estimation error are first characterized infinitesimally so to yield bounds on the rate of convergence and overshoot that depend on the parameters. By recasting the problem as the stabilization of a compact set, robustness properties of the proposed algorithm in the presence of disturbances in the system dynamics as well as measurement noise in the output are established. The proposed strategy is applied to spacecraft relative motion control with position-only measurements.**

I. Introduction

The Kalman filter and its variants are among the most widely used estimation techniques in real-world applications in the presence of limited sensor data. Due to advances in the field of nonlinear observer design in recent times (see [1], [2] and the references therein), there have been a renewed interest in modeling Kalman filters as high gain observers. For this purpose, several strategies have been suggested for transforming an extended Kalman filter into an adaptive high-gain observer [3]. To keep the observer design more realistic, a continuous-discrete version of the high-gain extended Kalman filter for a control affine system with periodic measurements was explored in [4] and multi-rate sampling is presented in [5]. These observers are based on a canonical form of uniformly observable systems and present a solution-based approach to demonstrate the stability of the error dynamics under global Lipschitz assumptions. In additon, [5] presents the results on preservation of observability under multi-rate sampling. Most recently, in [6], a Luenberger-like version of these high-gain observers for interconnected systems was presented in the hybrid system framework [7]. In contrast to the above mentioned high-gain techniques in which, the correction gain associated with the new measurement is obtained by integrating a continuous-discrete time Riccati equation, the results in [8] and [9] consider a constant correction term with uniform and nonuniform sampled measurements respectively. Extending similar ideas to linear continuous-discrete time networked control systems, [10] presents observer design with various static and dynamic time-scheduling protocols. A trajectory-based stability analysis is presented using small-gain arguments. For state affine systems, [11] presents a continuous-discrete observer that establishes exponential stability property for the error dynamics with a regularly persistent input. A similar continuous-discrete observer with variable sampling period for measurements is presented in [12].

In this paper, we propose an extended Kalman filter (without high-gain) in its deterministic form with hybrid dynamics and present its associated stability analysis. More precisely, we propose an extended Kalman filter with nonuniform sampled measurements generating an estimate that changes discretely, when the information arrives, and also continuously in between such events. Particularly, in contrast to [5], where, a time varying output matrix formulation is used to represent nonuniform sampled measurements, we consider a constant output matrix. In addition, our results allow for the measurements of the output of the plant to be only available intermittently, thus only allowing the observer to update the estimates of the state at aperiodic time instances within a window. We present sufficient conditions involving the parameters defining that window to achieve convergence of the error to zero using a Lyapunov analysis for hybrid systems. Further, we also show that the proposed hybrid Kalman filter is robust to measurement noise in the outputs and perturbations associated with the system dynamics by presenting input-to-state stability analysis.

This work is motivated by the recent advances in applying hybrid system theory for formation flying of spacecraft and proximity operations (e.g. rendezvous and docking) [13]. In [14] and in [15] the authors have shown that considering the full nonlinear dynamics of the spacecraft will results in improved state estimation in otherwise weakly observable or unobservable linear models. Hence, we consider linearized spacecraft relative motion equations and apply our hybrid Kalman filter to estimate the state from aperiodic position measurements. In addition, for this application, the spacecraft is to be controlled via thrusters similar to the ideas presented in [13].

The remainder of this paper is organized as follows. The notation used in paper is in Section I-A. In Section II, we state the problem along with preliminaries on hybrid systems and propose an observer design. The hybrid model of the closed-loop system and its stability analysis are discussed in Section III. A robustness analysis for the closed-loop system is considered in Section III-D. Numerical results for the relative orbit estimation of a follower spacecraft relative to a target in a reference circular orbit using position-only measurements is in Section IV. Proofs of the results will be published elsewhere.

A. Notation

The following notation and definitions are used throughout the paper. $\mathbb{R}$ denotes the real numbers. $\mathbb{R}^n$ denotes n-dimensional Euclidean space. $\mathbb{Z}$ denotes the integers. $\mathbb{R}_{\geq 0}$

B. P. Malladi, E. A. Butcher are with the Department of Aerospace and Mechanical Engineering, University of Arizona, 1130 N Mountain Ave, Tucson, AZ, 85721. email: malladi@email.arizona.edu, email: ebutcher@email.arizona.edu

R. G. Sanfelice is with the Department of Computer Engineering, University of California at Santa Cruz, 1156 High Street MS:SOE3, Santa Cruz, CA 95064. email: ricardo@ucsc.edu.

This research has been partially supported by the National Science Foundation under CAREER Grant no. ECS-1450484, Grant no. ECS-1710621, and Grant no. CNS-1544396, by the Air Force Office of Scientific Research under Grant no. FA9550-16-1-0015, by the Air Force Research Laboratory under Grant no. FA9453-16-1-0053, and by CITRIS and the Banatao Institute at the University of California.

denotes the nonnegative real numbers, i.e., $\mathbb{R}_{\geq 0} = [0, \infty)$. $\mathbb{N}$ denotes the natural numbers including 0, i.e., $\mathbb{N} = \{0, 1, \ldots\}$. $\Pi_{\geq 0}$ and $\Pi_{>0}$ denote the set of positive semidefinite and positive definite, symmetric matrices, respectively. Given a set $\mathcal{A} \subset \mathbb{R}^n$ and a point $x \in \mathbb{R}^n$, $|x|_{\mathcal{A}} := \inf_{y \in \mathcal{A}} |x - y|$. The equivalent notation $[x^\top \; y^\top]^\top$ and (x, y) is used for vectors, $x, y \in \mathbb{R}^n$. Given a vector $y \in \mathbb{R}^n$, $|y|$ denotes its Euclidean norm. For a generic vector norm $|.|$, its corresponding induced matrix norm on P is given by $|P|$. Given a symmetric positive matrix P, $\lambda(P)$ denotes its eigenvalue. I denotes an identity matrix of appropriate dimension. I_s denotes the s-dimensional identity matrix. A function $\alpha : \mathbb{R}_{\geq 0} \to \mathbb{R}_{\geq 0}$ is said to belong to class-$\mathcal{K}$ if it is continuous, zero at zero, and strictly increasing. A function $\alpha : \mathbb{R}_{\geq 0} \to \mathbb{R}_{\geq 0}$ is said to belong to class-$\mathcal{K}_\infty$ if it belongs to class-$\mathcal{K}$ and is unbounded. A function $\beta : \mathbb{R}_{\geq 0} \times \mathbb{R}_{\geq 0} \to \mathbb{R}_{\geq 0}$ is said to belong to class-$\mathcal{KL}$ if it is nondecreasing in its first argument, nonincreasing in its second argument, and $\lim_{s \searrow 0} \beta(s, t) = \lim_{t \to \infty} \beta(s, t) = 0$.

II. Problem statement

A. System design

In this paper, we consider control affine nonlinear systems of the form

$$\left.\begin{array}{rcl} \dot{\eta} & = & f(\eta) + \sum_{i=1}^{p} \xi_i(\eta) u_i \\ y & = & h(\eta) \end{array}\right\} \quad \eta \in \mathbb{R}^n, u_i \in \mathbb{R} \tag{1}$$

where $f : \mathbb{R}^n \to \mathbb{R}^n$, $\xi_i : \mathbb{R}^n \to \mathbb{R}^n$, $y \in \mathbb{R}^r$ is the measured output, and $h : \mathbb{R}^n \to \mathbb{R}^r$, that can be written in the normal form

$$\begin{array}{rcll} \dot{\eta}_1 & = & \eta_2 & + \sum_{i=1}^{p} \xi_{1,i}(\eta_1) u_i \\ \dot{\eta}_2 & = & \eta_3 & + \sum_{i=1}^{p} \xi_{2,i}(\eta_1, \eta_2) u_i \\ & \vdots & & \\ \dot{\eta}_{N-1} & = & \eta_N & + \sum_{i=1}^{p} \xi_{N-1,i}(\eta_1, \eta_2, \ldots, \eta_{N-1}) u_i \\ \dot{\eta}_N & = & \varphi(\eta) & + \sum_{i=1}^{p} \xi_{N,i}(\eta_1, \eta_2, \ldots, \eta_{N-1}, \eta_N) u_i \\ y & = & \eta_1 & \end{array} \tag{2}$$

on $\mathbb{R}^r$, where $\eta = (\eta_1, \eta_2, \ldots, \eta_N)$, $N \in \mathbb{N}_{\geq 0}$, $\eta_i \in \mathbb{R}^r$ for each $i \in \{1, 2, \ldots, N\}$, and the functions $\varphi : \mathbb{R}^n \to \mathbb{R}^r$, $\xi_{N,i} : \mathbb{R}^n \to \mathbb{R}^r$, $i \in \{1, 2, \ldots, p\}$ are globally Lipschitz. Note that such a transformation and the properties of the associated functions can also be considered on an open subset $\Omega \subset \mathbb{R}^r$ if a normal form exists on it, but for simplicity we work on $\mathbb{R}^r$. System (2) can be compactly written as

$$\begin{array}{rcl} \dot{\eta} & = & A\eta + b(\eta, u) \\ y & = & H\eta \end{array} \tag{3}$$

where

$$A := \begin{bmatrix} 0 & I_r & 0 \ldots & 0 \\ & \vdots & & \\ 0 & \ldots & 0 & I_r \\ 0 & \ldots & 0 & 0 \end{bmatrix},$$

is a $Nr \times Nr = n \times n$ block-antishift matrix,

$$H : \mathbb{R}^n \to \mathbb{R}^r = \begin{bmatrix} I_r & 0 & \ldots & 0 \end{bmatrix},$$

$b(\eta, u)$ is lower block-triangular; k^{th} component of b_k depends only on $(\eta_1, \eta_2, \ldots, \eta_k)$ and the components $(\eta, u) \mapsto b_k(\eta, u)$ are compactly supported with respect to all their η arguments. The existence of the normal form (3) requires the nonlinear system (1) to have specific observability properties, including instantaneously uniform and strong differential observability; see [16], [1].

Let $t \mapsto \eta(t)$ be a solution to the system (3) on $\mathbb{R}^r$ an input $u \in \mathcal{U}$, where $\mathcal{U}$ is a set of measurable functions with values in $U \subset \mathbb{R}^p$ that are bounded on any subset of $[0, \infty)$. For each such (η, u), we define $t \mapsto \widetilde{A}(t)$ as the linearization of (3). To this function, we associate the following family of linear time-varying systems with state $\zeta \in \mathbb{R}^n$ and input $\nu \in \mathbb{R}^p$:

$$\dot{\zeta} = \widetilde{A}(t)\zeta + \widetilde{B}(t)\nu, \tag{4}$$

where $\widetilde{A}(t) := A + \frac{\partial b}{\partial \eta}(\eta(t), u(t))$, and $\widetilde{B}(t) = \frac{\partial b}{\partial u}(\eta(t), u(t))$ for all $t \geq 0$. Below, Ψ_η denotes the state transition matrix for (4) that satisfies

$$\frac{d\Psi_\eta(t, s)}{dt} = \widetilde{A}^\top(t) \Psi_\eta(t, s), \quad \Psi_\eta(s, s) = I. \tag{5}$$

for all $(t, s) \in \mathbb{R}_{\geq 0} \times \mathbb{R}_{\geq 0}$. Next, we consider the following assumptions.

Assumption 2.1: Given the normal form (3), there exists $\overline{\tau} > 0$ such that for each $\eta \in \mathbb{R}^r$ there exists $\epsilon > 0$ such that

$$\int_0^{\overline{\tau}} \Psi_\eta(t, \overline{\tau})^\top H^\top H \Psi_\eta(t, \overline{\tau}) dt \geq \epsilon I, \tag{6}$$

where $\Psi_\eta(t, s)$ for all $t, s \in [0, \overline{\tau}]$ is given in (5).

Assumption 2.2: The input $u \in \mathcal{U}$ is bounded and the function $(\eta, u) \mapsto b(\eta, u)$ is globally Lipschitz uniformly in u. In particular, there exists $L \geq 0$ such that $|b(\eta_1, u) - b(\eta_2, u)| \leq L|\eta_1 - \eta_2|$ for any $\eta_1, \eta_2 \in \mathbb{R}^n$ and any $u \in \mathcal{U}$.

Assumption 2.1 requires uniform infinitesimal observability (or uniform reconstructibility) of the normal form (3). This property holds for free (and actually uniformly on ϵ) for systems in such normal form with a bilinear nonlinearity b; see [1, Lemma 2.11]. Essentially, this assumption guarantees a lower and upper bound on the information matrix of the Kalman filter; see [17, Proposition 2.2 and Proposition 2.4].

For the systems satisfying the assumptions above, we propose a Kalman-like hybrid observer that guarantees an explicit $\mathcal{KL}$ bound on the estimation error in terms of the parameters for all (hybrid) time instances in the domain of definition of the trajectories.

B. Well-posed hybrid systems

Hybrid systems are dynamical systems with both continuous and discrete dynamics. In this paper, we consider the framework for hybrid systems outlined in [7], [18], where a hybrid system $\mathcal{H} = (C, f, D, g)$ is defined by the following objects: a map $f : \mathbb{R}^n \to \mathbb{R}^n$ called the *flow map*; a map $g : \mathbb{R}^n \to \mathbb{R}^n$ called the *jump map*; a set $C \subset \mathbb{R}^n$ called the *flow set*; and a set $D \subset \mathbb{R}^n$ called the *jump set*. The flow map f defines the continuous dynamics on the flow set C, while the jump map g defines the discrete dynamics on the jump set D. These objects are referred to as the data of the hybrid system $\mathcal{H}$. Given a state χ of the hybrid system $\mathcal{H}$, the notation χ^+ indicates the values of the state after the jump[1]. A solution ϕ to $\mathcal{H}$ is given on extended time domain, called *hybrid time domain*, that is parametrized by the pairs (t, j), where t is the ordinary time component and j is a discrete parameter that keeps track of the number of jumps; see [7, Definition 2.6]. Given a solution ϕ to $\mathcal{H}$, the notation $\operatorname{dom}\phi$ represents its domain, which is a hybrid time domain. A solution to $\mathcal{H}$ is said to be *nontrivial* if $\operatorname{dom}\phi$ contains at least one point different from $(0, 0)$, *complete* if $\operatorname{dom}\phi$ is unbounded, and *maximal* if it cannot be extended, i.e., it is not a truncated version of another solution. The set $\mathcal{S}_{\mathcal{H}}(\xi)$ denotes the set of all maximal solutions to $\mathcal{H}$ from ξ. This framework also permits explicit modeling of perturbations in the system dynamics, a feature that is very useful for robust stability analysis of dynamical systems; see [7] for more details.

C. Observer design

Given system (3), the measurements of $y = h(\eta)$ are available intermittently at time instances t_k, $k \in \mathbb{N}$ that are separated by $\tau \in [T_{\min}, T_{\max}]$ seconds, where $0 < T_{\min} \leq T_{\max}$. The scalars $T_{\min}$ and $T_{\max}$ define the lower and upper bounds, respectively, for the time in between the measurement events. These dynamics implement the following mechanism: whenever the timer τ reaches an arbitrary value in the closed set $[T_{\min}, T_{\max}]$, a new measurement is available and the timer is reset back to zero from where it counts towards $[T_{\min}, T_{\max}]$ again. The dynamics for the timer τ are given by the hybrid model

$$\begin{array}{rcll} \dot{\tau} & = & 1 & \tau \in [0, T_{\max}], \\ \tau^+ & = & 0 & \tau \in [T_{\min}, T_{\max}]. \end{array} \tag{7}$$

With the availability of a new measurement $y \in \mathbb{R}^r$, motivated by the results in [1], [3], [19], we propose the following hybrid observer with state $\chi_c := (\eta_c, S, \tau) \in \mathbb{R}^n \times \Pi_{\geq 0} \times [0, T_{\max}] =: X_c$

$$\begin{array}{rcllll} \dot{\chi}_c & = & f_c(\chi_c, u) & (\chi_c, u) & \in & C_c \times U, \\ \chi_c^+ & = & g_c(\chi_c) & \chi_c & \in & D_c, \end{array} \tag{8}$$

where the maps $f_c : X_c \times U \to X_c$, $g_c : X_c \to X_c$ and the sets $C_c \subset X_c$, $D_c \subset X_c$ are

$$f_c(\chi_c, u) := \begin{bmatrix} A\eta_c + b(\eta_c, u) \\ -\widetilde{A}^\top S - S\widetilde{A} - SQS \\ 1 \end{bmatrix} \forall (\chi_c, u) \in C_c \times U,$$

$$g_c(\chi_c) := \begin{bmatrix} \eta_c + (\star_3)^{-1} H^\top (\frac{R}{\tau})^{-1}(y - h(\eta_c)) \\ \star_3 \\ 0 \end{bmatrix} \forall \chi_c \in D_c,$$

$C_c := \mathbb{R}^n \times \Pi_{\geq 0} \times [0, T_{\max}]$, $D_c := \mathbb{R}^n \times \Pi_{\geq 0} \times [T_{\min}, T_{\max}]$; with a slight abuse of notation $\widetilde{A} := A + \frac{\partial b}{\partial \eta_c}(\eta_c, u)$, as defined below (4), $\star_3 := S + H^\top (\frac{R}{\tau})^{-1} H$; the $Q \in \Pi_{>0}$ and $R \in \Pi_{>0}$ are similar to the covariance matrices of the state noise and output noise in the stochastic context, respectively.

The components of the observer state χ_c consist of the estimated system state η_c, the error information matrix S, and a timer τ that triggers measurement errors at isolated time instances t_k, $k \in \mathbb{N}$. In addition, the input $u \in \mathcal{U}$ is available to the observer, i.e., the input is not sampled.

Note that the hybrid observer dynamics given in (8) resemble the continuous-discrete extended Kalman filter presented in [1, Section 2.4.4] but without high gain. In paticular, the flow dynamics (f_c, C_c) resemble the 'prediction step' given in [1, equation (104)] and the jump dynamics (g_c, D_c) resemble the 'innovation step' [1, equation (105)]. In addition to adapting the extended Kalman filter formulation into a hybrid system framework, the observer proposed in (8) incorporates a time window $[T_{\min}, T_{\max}]$, as opposed to the periodic measurement updates in [1] and time varying output matrix to represent aperiodic measurement updates in [5]. Such mechanism is explicitly modeled as part of the dynamics of the hybrid system. In [12], a continuous-discrete observer for a state affine system is designed based on variable sampling time that is used as a tuning parameter to compute measurement time online resembling an event-triggered methodology. In contrast, the observer proposed in (8) accommodates sporadic sensor measurements for uniformly observable systems.

[1]Precisely $\chi^+ = \chi(t, j+1)$ or $\chi^+ = g(\chi(t, j))$

III. Stability properties of the Hybrid Closed-loop System

To estimate the state $\eta \in \mathbb{R}^n$ from the intermittent measurements $y \in \mathbb{R}^r$, we consider the plant model in (3) interconnected with the observer given in (8). The resulting hybrid closed-loop system $\mathcal{H} := (C, f, D, g)$ has state $\chi := (\eta, \eta_c, S, \tau) \in \mathbb{R}^n \times X_c =: X$ and dynamics given by

$$\begin{array}{rcllll} \dot{\chi} & = & f(\chi, u) & (\chi, u) & \in & C \times U, \\ \chi^+ & = & g(\chi) & \chi & \in & D, \end{array} \tag{9}$$

where $f : X \times U \to X$, $g : X \to X$ and the sets $C \subset X$, $D \subset X$ are

$$f(\chi, u) := \begin{bmatrix} A\eta + b(\eta, u) \\ A\eta_c + b(\eta_c, u) \\ -\widetilde{A}^\top S - S\widetilde{A} - SQS \\ 1 \end{bmatrix} \quad \forall\ (\chi, u) \in C \times U,$$

$$g(\chi) := \begin{bmatrix} \eta \\ \eta_c + (\star_3)^{-1} H^\top (\frac{R}{\tau})^{-1}(y - h(\eta_c)) \\ \star_3 \\ 0 \end{bmatrix} \quad \forall\ \chi \in D,$$

$C := \mathbb{R}^n \times C_c$, $D := \mathbb{R}^n \times D_c$.

With the construction above, the hybrid closed-loop system $\mathcal{H}$ satisfies the following property.

Lemma 3.1: The hybrid system $\mathcal{H}$ satisfies the hybrid basic conditions, i.e.,

- *(A1) C and D are closed subsets of X.*
- *(A2) $f : X \times U \to X$ is continuous.*
- *(A3) $g : X \to X$ is continuous.*

Next, we consider the following property on the timer τ.

Lemma 3.2: Given a solution ϕ to $\mathcal{H}$, let t_j be defined such that a jump occurs at $(t_j, j-1)$ with $j \in \mathbb{N} \setminus \{0\}$. Then,

$$j \leq 1 + \frac{t}{T_{\min}} \tag{10}$$

for all $(t, j) \in \operatorname{dom}\phi$, $j \geq 1$.

A. Error Dynamics

The set of interest for closed-loop hybrid system $\mathcal{H}$ in (9) is the closed set

$$\mathcal{A} := \{\chi \in X : e = 0, \tau \in [0, T_{\max}]\}, \tag{11}$$

where $e := \eta - \eta_c$. The dynamics of $e \in \mathbb{R}^n$ from (9) are hybrid and given by

$$\begin{array}{lll} \dot{e} & = \dot{\eta} - \dot{\eta}_c = Ae + b(\eta, u) - b(\eta_c, u) & (\chi, u) \in C \times U, \\ e^+ & = e - (\star_3)^{-1} H^\top (\frac{R}{\tau})^{-1} He & \chi \in D, \end{array} \quad (12)$$

here $C := \mathbb{R}^n \times C_c$, $D := \mathbb{R}^n \times D_c$, the flows occur when the timer $\tau \in [0, T_{\max}]$ and jumps occur when $\tau \in [T_{\min}, T_{\max}]$.

First, we provide a matrix version of [1, Lemma 2.21] which will be used to derive the results in this paper.

Lemma 3.3: If $P = S^{-1}$ is a symmetric positive definite matrix, $R \in \Pi_{>0}$ and $\tau > 0$, then

$$(P + PH^\top (\tfrac{R}{\tau})^{-1} HP)^{-1} = P^{-1} - H^\top (HPH^\top + \tfrac{R}{\tau})^{-1} H.$$

In addition, the following infinitesimal properties of the function $V : \chi \mapsto \mathbb{R}_{\geq 0}$, will be used for the main result presented in Section III-C.

Proposition 3.4: Given the hybrid error dynamics $e \in \mathbb{R}^n$ in (12), and the dynamics of S in (9) with $S \in \Pi_{>0}$ the function

$$V(\chi) := e^\top S e \quad (13)$$

has the following infinitesimal properties:

- *for all $\chi \in C \setminus \mathcal{A}$, $u \in U$,*
$$\langle \nabla V(\chi), f(\chi, u) \rangle = e^\top (-SQS)e + 2e^\top S(b(\eta, u) - b(\eta_c, u) - b^*(\eta_c, u)e),$$
where $b^* = \frac{\partial b}{\partial \eta_c}$.
- *for all $\chi \in D \setminus \mathcal{A}$,*
$$V(g(\chi)) - V(\chi) = -e^\top (H^\top (HS^{-1}H^\top + R/\tau)^{-1} H)e.$$

B. Analysis of S Component of Solutions

To establish a desired stability result for the hybrid closed-loop system (9), we perform the following analysis on the S component of its solution $\phi := (\phi_\eta, \phi_{\eta_c}, \phi_S, \phi_\tau)$.

Assumption 3.5: The constants $T_{\min}, T_{\max}$, the matrix $\widetilde{A} := A + \frac{\partial b}{\partial \eta_c}(\eta_c, u)$, and the positive definite symmetric matrices Q, R satisfy the following conditions: and there exists positive constants $a, \underline{q}, \overline{q}, \underline{r}, \overline{r}$ such that

1) $|\widetilde{A}| \leq a \quad \forall (\eta_c, u) \in \mathbb{R}^n \times U$
2) $0 < \underline{q} I \leq Q \leq \overline{q} I$
3) $0 < \underline{r} I \leq R \leq \overline{r} I$
4) $0 < T_{\min} \leq T_{\max}$

Lemma 3.6: Suppose Assumption 3.5 holds, and that a positive real number $0 < k_1 < k_2 := 4a/\underline{q}$ and a compact set

$$K \subset \{S \in \Pi_{\geq 0} : k_1 I \leq S \leq k_2 I\},$$

are given. Let the positive real number $\overline{\tau}$ satisfy the condition (6) *in Assumption 2.1. Let ϕ_S be the S component of the maximal solution ϕ to the hybrid system $\mathcal{H}$ from $\phi(0,0) \in \mathbb{R}^n \times \mathbb{R}^n \times K \times [0, T_{\max}]$. Then the solution ϕ is complete and during flows, i.e., for each $j \in \mathbb{N}$ such that $I^j := \{t : (t, j) \in \operatorname{dom} \phi\}$ has nonempty interior, its S component satisfies*

$$\tilde{k}_1 I \leq \phi_S(t, j) \leq k_2 I, \quad (14)$$

for all $(t, j) \in \operatorname{dom} \phi$, where $\widetilde{k}_1 := k_1 \exp(-(k_2 \overline{q} + 2a)\overline{\tau})$.

Note that if the continuous dynamics of S include a term that is quadratic on H (see, e.g., [1, equation (91)]), the parameter $\epsilon > 0$ in (6) would play a role in quantifying the lower bound $\widetilde{k}_1$.

C. Stability

With the definitions of the hybrid system given in (9) and the set to stabilize in (11), our main result is as follows.

Theorem 3.7: Let the input $u \in \mathcal{U}$ and the function b satisfy Assumption 2.2 with $L > 0$. Suppose that the constants $T_{\min}, T_{\max}$, and that there exists positive constants $a, \underline{q}, \overline{q}, \underline{r}, \overline{r}$, such that the matrix $\widetilde{A} = A + \frac{\partial b}{\partial \eta}(\eta, u)$ and the positive definite symmetric matrices Q, R satisfy the conditions in Assumption 3.5. Let the positive real number $\overline{\tau}$ satisfy the condition (6) *in Assumption 2.1. Given a positive real number $0 < \tilde{k}_1 < k_1 < k_2 := 4a/\underline{q}$ and a compact set*

$$K \subset \{S \in \Pi_{\geq 0} : k_1 I \leq S \leq k_2 I\},$$

if $\tilde{k}_1 := k_1 \exp(-(k_2 \overline{q} + 2a)\overline{\tau})$ and k_2 are such that

$$\underline{q} \tilde{k}_1^2 > 4Lk_2, \quad (15)$$

and

$$T_{\max} < T_{\min} \left(1 + \frac{\underline{q} \tilde{k}_1^2 - 4Lk_2}{\sigma \tilde{k}_1} \right) \quad (16)$$

hold, where σ is any positive number sufficiently small to verify (16)*, then every $\phi \in \mathcal{S}_{\mathcal{H}}(\phi(0,0))$, where $\phi(0,0) \in \mathbb{R}^n \times \mathbb{R}^n \times K \times [0, T_{\max}]$, is complete and satisfies*

$$|\phi(t,j)|_{\mathcal{A}} \leq \beta(|\phi(0,0)|_{\mathcal{A}}, t + j) \quad (17)$$

$\forall (t, j) \in \operatorname{dom} \phi$, where β is a class-$\mathcal{KL}$ function given by

$$\beta(r, s) := {\alpha_1}^{-1}(\alpha_2(r) \exp(m - \gamma(s))) \quad \forall\, r, s \geq 0,$$

$m := \sigma T_{\max}$; $\gamma(s) := (\rho - \sigma \frac{T_{\max}}{T_{\min}})s$, $\alpha_1(s) := \tilde{k}_1 s$, $\alpha_2(s) := \exp(-\sigma T_{\max}) k_2 s$, for each $s \geq 0$; $\rho := \left(\underline{q}\tilde{k}_1 - \frac{4Lk_2}{\tilde{k}_1}\right) + \sigma$.

Remark 3.8: From Theorem 3.7, every solution $\phi \in \mathcal{S}_{\mathcal{H}}(\phi(0,0))$, where $\phi(0,0) \in \mathbb{R}^n \times \mathbb{R}^n \times K \times [0, T_{\max}]$ to the closed-loop system in (9) is bounded and does not blow up in finite time. Also, $g(D) \subset C \cup D$ which shows that every solution ϕ to system $\mathcal{H}$ do not jump out of $C \cup D$. Therefore, since conditions (b) and (c) in [7, Proposition 6.10] are not satisfied, we conclude that every maximal solution to the closed-loop system $\mathcal{H}$ is complete.

D. Input-to-state-stability

To take our stability analysis close to the real world problems, let us consider that the plant (9) is effected by unmodeled dynamics given by $d_1 \in \mathbb{R}^{n \times 1}$, actuator error $d_2 \in \mathbb{R}^{p \times 1}$ as following

$$\dot{\eta} = f(\eta, u + d_2) + d_1.$$

We also consider that the measurement noise $d_3 \in \mathbb{R}^{r \times 1}$ is added to the output,

$$y = h(\eta) + d_3.$$

Then, denoting by d the signals d_i, $i \in \{1, 2, 3\}$ extended to the state space of $\chi := (\eta, \eta_c, S, \tau) \in X$, the closed loop system $\mathcal{H}$ in (9) results in the perturbed closed-loop system $\mathcal{H}_d$ with dynamics

$$\begin{array}{lll} \dot{\chi} & = f_d(\chi, u + d_2) + d_p & (\chi, u + d_2) + d_p \in C_d \times U, \\ \chi^+ & = g_d(\chi, y + d_3) & (\chi, y + d_3) \in D_d \times \mathbb{R}^r, \end{array} \quad (18)$$

here $d_p := [d_1 \quad 0_{n\times 1} \quad 0_{n\times n} \quad 0]^\top$, the maps $f_d : X\times U \to X$, $g_d : X\times \mathbb{R}^r \to X$ and the sets $C_d \subset X$, $D_d \subset X$, respectively. Next, we show that the semiglobal-asymptotic stability of the compact set $\mathcal{A}$ in (11) for the hybrid system $\mathcal{H}_d$ in (18) is robust to perturbations and is input-to-state stable (ISS), namely

Definition 3.9: A hybrid system $\mathcal{H}_d$ with input d is input-to-state-stable with respect to $\mathcal{A}$ if there exists $\beta \in \mathcal{KL}$ and $\kappa \in \mathcal{K}$ such that each solution pair (ϕ, d) to $\mathcal{H}$ satisfies

$$|\phi(t,j)|_{\mathcal{A}} \le \max\{\beta(|\phi(0,0)|_{\mathcal{A}}, t+j), \kappa(|d|_{(t,j)})\}. \quad (19)$$

To establish ISS result, let us first consider the following assumption on the input with perturbations.

Assumption 3.10: The input $u \in \mathcal{U}$ and input perturbation $t \mapsto d_2(t) \in \mathbb{R}^p$ are bounded and the function $(\eta, u+d_2) \mapsto b(\eta, u+d_2)$ is globally Lipschitz uniformly in $u+d_2$. In particular, there exists $L \ge 0$ such that $|b(\eta_1, u+d_2) - b(\eta_2, u+d_2)| \le L|\eta_1 - \eta_2|$ for any $\eta_1, \eta_2 \in \mathbb{R}^n$.

Theorem 3.11: Let the input $u \in \mathcal{U}$ and the function b satisfy Assumption 3.10 with $L > 0$. Suppose that the constants $T_{\min}, T_{\max}$, and that there exists positive constants $a, \underline{q}, \overline{q}, \underline{r}, \overline{r}$, such that the matrix $\widetilde{A} = A + \frac{\partial b}{\partial \eta_c}(\eta_c, u)$ and the positive definite symmetric matrices Q, R satisfy the conditions in Assumption 3.5. Let the positive real numbers $\overline{\tau}$ satisfy the condition (6) *in Assumption 2.1. Given positive real numbers $0 < \tilde{k}_1 < k_1 < k_2 := 4a/\underline{q}$ and a compact set $K \subset \{S \in \Pi_{\ge 0} : k_1 I \le S \le k_2 I\}$, if $\tilde{k}_1 := k_1 \exp(-(k_2\overline{q} + 2a)\overline{\tau})$ and k_2 are such that* (15)*, and* (16) *hold, where σ is any positive number sufficiently small to verify* (16)*, then the hybrid system $\mathcal{H}_d$ with input is ISS with respect to the set $\mathcal{A}$, namely, for each solution pair (ϕ, d) with $\phi \in \mathcal{S}_{\mathcal{H}}(\phi(0,0))$, where $\phi(0,0) \in \mathbb{R}^n \times \mathbb{R}^n \times K \times [0, T_{\max}]$ satisfies* (19)*, and β is a class-$\mathcal{KL}$ function given by*

$$\beta(r,s) := {\alpha_1}^{-1}(\alpha_2(r)\exp(m - \gamma(s))) \quad \forall\, r, s \ge 0,$$

$m := \sigma T_{\max} + \ln 2$, $\rho := \left(\underline{q}\tilde{k}_1 - \frac{4Lk_2}{\tilde{k}_1}\right) + \sigma$ and for each $s \ge 0$, $\gamma(s) := (\rho - \sigma\frac{T_{\max}}{T_{\min}})s$, $\alpha_1(s)$, $\alpha_2(s)$ are class-$\mathcal{K}_\infty$ functions, the class-$\mathcal{K}$ function κ is given by

$$\kappa(r) := {\alpha_1}^{-1}(\alpha_2(\max\{a_1, a_2, a_3\}r)) \qquad \forall\, r \ge 0,$$

that holds for input $|d|_{(t,j)}$, where $a_1 := \sqrt{\exp(\sigma T_{max})\left(\frac{\gamma_1 + 4\gamma_2\tilde{k}_1}{4\tilde{k}_1}\right)}$, $a_2 := \sqrt{\frac{2\exp(-\sigma T_{max})k_2}{\rho\tilde{k}_1}}$, $a_3 := \sqrt{\frac{\exp(-\sigma T_{max})k_2}{\rho 4L}}$.

IV. Application

A. Spacecraft Nonlinear Model

We consider a nonlinear model of relative circular motion of a chaser spacecraft relative to a target spacecraft resolved in the local vertical local horizontal frame (denoted by H) (see [20, Chapter 14] for more details) given by

$$\begin{aligned}\tfrac{d^2}{dt^2}(\vec{r}^H) = &-2\vec{\omega}^H \times \vec{v}^H - \vec{\omega}^H \times (\vec{\omega}^H \times \vec{r}^H) \\ &+ \tfrac{\mu \vec{r}_c}{\|\vec{r}_c\|^3} - \tfrac{\mu \vec{r}_d^H}{\|\vec{r}_d^H\|^3} + \vec{u}^H\end{aligned} \quad (20)$$

where $\vec{r}_c := (r_o, 0, 0) \in \mathbb{R}^3$, $\vec{r}^H := (x, y, z) \in \mathbb{R}^3$ and $\vec{v}^H := (\dot{x}, \dot{y}, \dot{z}) \in \mathbb{R}^3$ are position and velocity, respectively, r_o is the orbit radius of the target spacecraft, $\vec{u}^H := \frac{1}{m_c}(F_x, F_y, F_z) \in \mathbb{R}^3$ is the input with F_x, F_y and F_z, the control forces in the x, y and z directions, m_c is the mass of the chaser, $\vec{\omega}^H := (0,0,n)^\top$, $n := \sqrt{\frac{\mu}{{r_o}^3}}$ where μ is the gravitational parameter of the Earth, $\vec{r}_d^H := (r_o + x, y, z) \in \mathbb{R}^3$ and $\|\vec{r}_d^H\| = \sqrt{(r_o+x)^2 + y^2 + z^2}$. In addition, the input $\vec{u}^H$ has a maximum thrust constraint $\|\vec{u}^H\| \le u_{max}$, $u_{max} > 0$.

1) Position only measurements: With position only measurements, the linearized spacecraft equations in (20) are in the desired normal form given by

$$\begin{aligned}\dot{\eta} &= A\eta + b(\eta, u) \\ y &= C\eta\end{aligned} \quad (21)$$

where the state vector $\eta := (\vec{r}^H, \vec{v}^H) \in \mathbb{R}^6$. The block-antishift matrix and the output matrices are

$$A = \begin{bmatrix} 0_{3\times 3} & I_{3\times 3} \\ 0_{3\times 3} & 0_{3\times 3}\end{bmatrix}, \quad C = [I_{3\times 3} \quad 0_{3\times 3}],$$

respectively. The lower block-triangular function $b(\eta, u) := A_d\eta + \frac{1}{m_c}Bu$,

$$A_d := \begin{bmatrix} & 0_{3\times 3} & & & 0_{3\times 3} & \\ 3n^2 & 0 & 0 & 0 & 2n & 0 \\ 0 & 0 & 0 & -2n & 0 & 0 \\ 0 & 0 & -n^2 & 0 & 0 & 0 \end{bmatrix}, B := \begin{bmatrix} & 0_{3\times 3} & \\ 1 & 0 & 0 \\ 0 & 1 & 0 \\ 0 & 0 & 1\end{bmatrix},$$

The system dynamics in (21) is linear, observable and in the normal form (3) thus satisfying Assumption 2.1 and with maximum thrust constrain $\|\vec{u}^H\| \le u_{max}$, $u_{max} > 0$, satisfies the Assumption 2.2, respectively. Note that that the linearized equation of motion (21) represent the so-called Clohessy-Wiltshire-Hill equations. Since $r_o < r_d$, for all $\eta, \eta_c \in \mathbb{R}^6$, the lower block triangular terms of the spacecraft linearized equations are bounded by $|b(\eta, u) - b(\eta_c, u)| \le L|\eta - \eta_c|$, where $L \approx 2n = 0.0021$. To estimate the state η from position ($\vec{r}^H$) only measurements, we implement a hybrid observer presented in (9) on the resulting plant. Next, we design a feedback controller, to which the state estimates η_c is fed similar to the controller design presented in [13].

2) Simulations: To simulate the spacecraft dynamics, we use $n = \sqrt{\frac{\mu}{{r_o}^3}}$, $\mu = 3.986 \times 10^{14}\frac{m^3}{s^2}$, $r_o = 7100000m$, $m_c = 500Kg$ in the simulations. In these simulations, the chaser starts at a distance of no more than $\rho_{\max} = 10Km$ away from the target. In addition, the thrusters have a maximum input of $u_{max} = 0.02m/sec^2$. As we consider full nonlinear relative motion equations for our application, a process noise (zero-mean Gaussian noise) with variance $(10^{-3})^2$ is added to the system dynamics to compensate for any additional unmodeled dynamics. Next, to simulate position measurements, a zero-mean Gaussian noise with variance $(25m)^2$ is considered.

With these mission parameters, simulations for the entire closed-loop system are performed for the chaser starting from η corresponding to various initial conditions in the 10Km radius with a initial velocity $\rho(\dot{x}(0,0), \dot{y}(0,0), \dot{z}(0,0)) \in [0, 0.866m/sec]$. The initial condition for the estimated state is $\eta_c(0,0) := \eta(0,0) \pm [1000m \quad 1000m \quad 1000m \quad 0m/sec \quad 0m/sec]$. For the controller design, a LQR controller is implemented with appropriate parameters satisfying input constraint $\|u\|_\infty \le 0.02m/sec^2$.

With the choice of $T_{\min} = 2$sec, the parameter σ is chosen sufficiently small to verify equation (16) and $T_{\max} <$

$T_{\min}(1+2) \leq 6sec$. Following this analysis the measurements in the simulation are updated intermittently at time instances t_k, $k \in \mathbb{N}$ that are separated by $\tau \in [2sec \quad 6sec]$.

Figure 1 shows the induced norm of the information matrix S satisfies $0 < \tilde{k}_1 < k_1 < k_2 := 4a/\underline{q}$ for a simulation time of 12×10^3 seconds. The trajectories of the chaser spacecraft

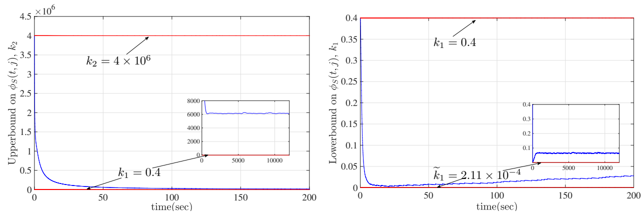

Fig. 1. Bounds on the information matrix $\phi_S(t,j) \in K$

for various initial conditions are shown in Figure 2, while the error, timer dynamics are presented in Figure 3. This shows that the hybrid Kalman filter works effectively to reduce the differences between the true and computed measurements for the estimated orbit in the presence of bounded inputs.

V. Conclusion

In this paper, a robust hybrid Kalman filter (in its deterministic form) with intermittent measurement data is presented. The problem of stabilizing the hybrid closed-loop system to a desired set was solved with assumptions on a certain normal form. Note that such an assumption can be relaxed by using high-gain formulation. Additionally, it was established that the hybrid system is robust to perturbations. We also quantified an upper bound on the perturbations and stabilized the origin of the closed-loop hybrid system to the desired set. These claims of robust stability are further illustrated by the simulation results on a spacecraft application with intermittent measurement data with the presence of process and measurement noise.

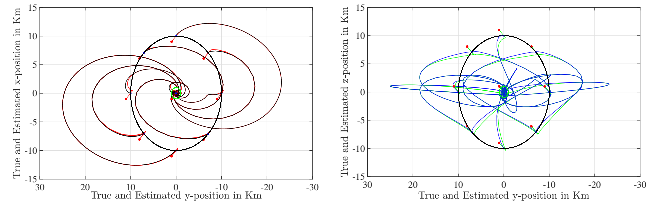

Fig. 2. Chaser true and estimated dynamics in XY and YZ, respectively

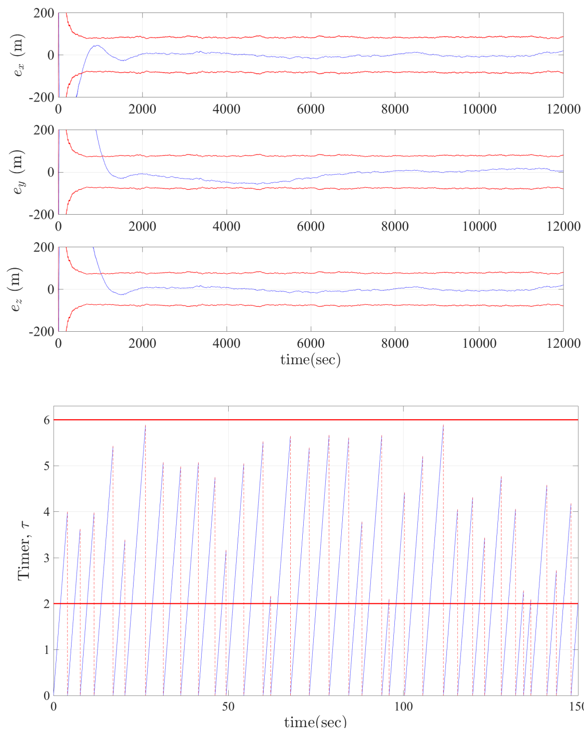

Fig. 3. Position estimate error (blue) and 5 - σ covariance matrix (P) bound (red) corresponding to the position-only estimation scenarios using full nonlinear dynamic models and timer dynamics with $\tau \in [2sec, 6sec]$

References

[1] J-P. Gauthier and I. Kupka. *Deterministic Observation Theory and Applications*. Cambridge University Press, 2001.

[2] G. Besançon. *Nonlinear observers and applications*, volume 363. Springer, 2007.

[3] N. Boizot, E. Busvelle, and J. P. Gauthier. An adaptive high-gain observer for nonlinear systems. *Automatica*, 46(9):1483–1488, 2010.

[4] N. Boizot. *Adaptative high-gain extended Kalman filter and applications*. PhD thesis, Université de Bourgogne; Université du Luxembourg, 2010.

[5] A. Feddaoui, N. Boizot, E. Busvelle, and V. Hugel. A Kalman filter for linear continuous-discrete systems with asynchronous measurements. In *Proceedings of 56th IEEE Conference on Decision and Control*, pages 2813–2818, December 2017.

[6] V. Andrieu, C. Prieur, S. Tarbouriech, and L. Zaccarian. A hybrid scheme for reducing peaking in high-gain observers for a class of nonlinear systems. *Automatica*, 72:138–146, 2016.

[7] R. Goebel, R. G. Sanfelice, and A. R. Teel. *Hybrid Dynamical Systems: Modeling, Stability, and Robustness*. Princeton University Press, New Jersey, 2012.

[8] T. N. Dinh, V. Andrieu, M. Nadri, and U. Serres. Continuous-discrete time observer design for Lipschitz systems with sampled measurements. *IEEE Transactions on Automatic Control*, 60(3):787–792, 2015.

[9] T. Raff, M. Kogel, and F. Allgower. Observer with sample-and-hold updating for Lipschitz nonlinear systems with nonuniformly sampled measurements. In *Proceedings of American Control Conference*, pages 5254–5257. IEEE, 2008.

[10] R. Postoyan and D. Nesic. A framework for the observer design for networked control systems. *IEEE Transactions on Automatic Control*, 57(5):1309–1314, 2012.

[11] M. Nadri and H. Hammouri. Design of a continuous-discrete observer for state affine systems. *Applied Mathematics Letters*, 16(6):967–974, 2003.

[12] V. Andrieu, M. Nadri, U. Serres, and J-C. Vivalda. Continuous discrete observer with updated sampling period. *IFAC Proceedings Volumes*, 46(23):439–444, 2013.

[13] B. P. Malladi, R. G. Sanfelice, E. Butcher, and J. Wang. Robust hybrid supervisory control for rendezvous and docking of a spacecraft. In *Proceedings of the 55th IEEE Conference on Decision and Control*, pages 3325 – 3330, December 2016.

[14] E. Kaufman, A. T. Lovell, and T. Lee. Nonlinear observability for relative orbit determination with angles-only measurements. *The Journal of the Astronautical Sciences*, 63(1):60–80, 2016.

[15] E. A Butcher, J. Wang, and A. T. Lovell. On Kalman filtering and observability in nonlinear sequential relative orbit estimation. *Journal of Guidance, Control, and Dynamics*, 40(9), 2017.

[16] J-P Gauthier, H Hammouri, and S Othman. A simple observer for nonlinear systems applications to bioreactors. *IEEE Transactions on automatic control*, 37(6):875–880, 1992.

[17] R. G. Sanfelice and L. Praly. Solution of a Riccati equation for the design of an observer contracting a Riemannian distance. In *Proceedings of the IEEE 54th Annual Conference on Decision and Control*, 2015.

[18] R. Goebel, R. G. Sanfelice, and A.R. Teel. Hybrid dynamical systems. *IEEE Control Systems Magazine*, 29(2):28–93, April 2009.

[19] R. G. Sanfelice and L. Praly. Convergence of nonlinear observers on $\mathbb{R}^n$ with a Riemannian metric (part ii). *IEEE Transactions on Automatic Control*, 61(10), October 2016.

[20] H. Schaub and J. L. Junkins. *Analytical mechanics of space systems*. AIAA, 2003.